Fracture Mechanics of Concrete Structures, de Borst et al (eds) © 2001 Swets & Zeitlinger, Lisse, ISBN 90 2651 825 0

Fracture Mechanics of Fibre-Reinforced Concrete: Material Modeling and Experimental Technique

O.Bayard & O.Plé
LMT, Cachan, France
A.Alvandl
ENS, Cachan, France

ABSTRACT: Reactive Powder Concrete (RPC) is made of very fine matrix with short steel fibres. The bridging fibre action increase the stress carried across the crack. To optimise the mechanical behaviour, the influence of the orientation of fibres due to the process of casting must be studied. By considering a locally oriented mass of fibres as an ellipsoidal inclusion embedded in an homogeneous medium of concrete, the Eshelby's inclusion model allows to obtain a description of the micro-structural strain concentration and to develop a model for crack initiation based on equivalent strain criterion. By using the micro-plane model coupled with damage theory we simulate the crack propagation in relation with the orientation of the fibres. Specimens of RPC with a given orientation of fibres, tested under uniaxial tension, confirm such a role-played by a locally anisotropic elastic behaviour on crack initiation, and on the bridging action during crack propagation.

1 INTRODUCTION

Reactive Powder Concrete (RPC) is a concrete of new generation with ultra high performances (Richard & Cheyrezy 1995a). Nevertheless, it remains in fragile matter. An improvement of ductility in a such high strength concrete can be obtained by adding straight short and metallic fibres (length: l_f= 13mm, diameter: d_f= 0.16mm).

When cracking appears on a very small scale, the fibres intervene to prevent a microcrack from being propagated. Under loading, the consequence is to multiply the microcracks before the propagation of a crack at the scale of the structure (propagation involving the ruin of the structure considered (Bentur & Mindess 1990)). During multi-cracking of material, action known as of « bridging » of cracks by fibres involves many micro mechanisms, which are more or less solicited according to the angle reigning between the direction of the local reinforcement (fibre) and the normal in the plane of cracking. Among these micro mechanisms, we meet the phenomena of bond and slip at the fibre-matrix interface (Bartos 1980, Bartos 1981, Gray 1984, Greszczuk 1969), of friction (Kelly & Zweben 1976, Pinchin & Tabor 1978), of bond-slip and pinching remotely called effect Cook-Gordon (Cook & Gordon 1964), as well as local moments related to the local bending of the fibre when it is tilted compared to the normal in the plan of cracking (Majumdar 1975).

The material (matrix and fibres) is heterogeneous. From this heterogeneity of the mechanical characteristics, the elastic fields within material before damage are disturbed by the presence of fibres. These fields within the matrix, as well as the transfers of load, which operate between fibres and the surrounding matrix, are not only function of the mechanical characteristics of each component, but also function of the local percentage out of fibres as well as local orientation of the fibrous reinforcement. In other words, the criterion of nucleation is dependent, with local scale (micro-scale), of the local percentage out of fibres and their orientation. Then the fibres control cracking (Fig. 1).

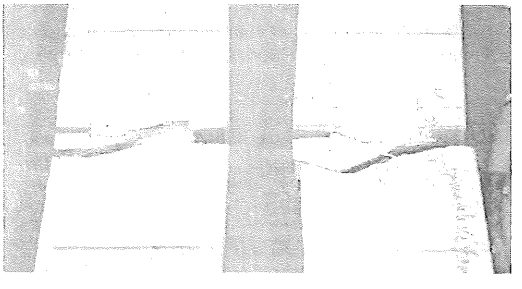

Figure 1. Fibres control cracking in samples with notches.

The nature of the fibrous suspension is that of a solution known as concentrated. That induce, as a consequence, a local alignment of fibres between them under effect of strong gradients of shearing and a regrouping of fibres by cluster, flow being no more

continuous but being done per blocks (Quemada 1986). Size of the clusters that we observe in experiments is approximately 20 to 40 mm according to the mode of casting (Fig. 2).

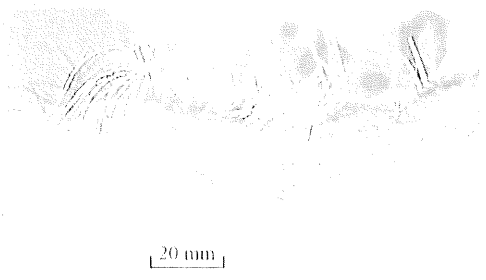

Figure 2. Cluster of aligned fibres.

It results a particular configuration for the distribution from fibres within the structure (Fig. 3b). If we regard a material as RPC, its usual field employment is that of the industry of structural elements with low dimensions and strong twinges. At this scale, the size of the structure is close to the size of the cluster of fibres. We are dealing with a composite consisting of two materials having its own laws of behaviour. For this study the authors propose to show the influence of an unspecified fibre distribution on the mechanical behaviour of a structure. With this intention, it was selected to break up the structure into "directed" cells (Fig. 3a). We will be interested in this article to describe and model the behaviour of such a cell (assembly will not be discussed here). This theoretical analysis is compared with a second analysis on samples of RPC. Specific specimens reinforced by oriented fibres have been tested under uniaxial tensile stress. The analysis of force-displacement curves and samples, after each test, have shown the influence of the oriented fibres.

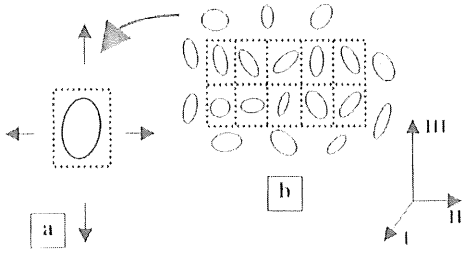

Figure 3. Fibres distribution shape :
a) Partial shape: isolated cell with cluster of aligned fibres.
b) Complete shape: assembled cells in interaction.

2 CELL UNDER UNIAXIAL TENSION IN ELASTICITY

2.1 *A locally oriented mass of fibres*

Let us consider a directed cell isolated from the remainder of the structure (Fig. 3a). It will be supposed that fibre cluster is a spheroid of twinge $r_0 = 3$ (Fig. 4). This fibre cluster being isolated from the other clusters, we consider it within a matrix of RPC without fibre. This problem is the problem of an ellipsoidal inclusion, modelled as a transversely isotropic medium, (Eshelby 1957, Mura 1982) embedded in an isotropic infinite medium of RPC (Fig. 4). The calculation of the rigidity of inclusion defined in the base {1,2,3} by the formulas of Christensen was programmed in computation software named SARAH, worked out on a Matlab basis. With the set of parameters { E_M = 50 GPa, ν_M = 0.18, E_f = 300 GPa, ν_f = 0.3 and a volume fraction of fibres, f equal to 2%}, we obtain the rigidity for the inclusion as:

$$R_I = 10^4 . \begin{pmatrix} 5.57 & 1.25 & 1.28 & 0 & 0 & 0 \\ 1.25 & 5.57 & 1.28 & 0 & 0 & 0 \\ 1.28 & 1.28 & 5.98 & 0 & 0 & 0 \\ 0 & 0 & 0 & 2.18 & 0 & 0 \\ 0 & 0 & 0 & 0 & 2.18 & 0 \\ 0 & 0 & 0 & 0 & 0 & 2.16 \end{pmatrix}_{\{1,2,3\}} \quad (1)$$

The formulations with this type of problem were presented within the framework of preceding articles (Bayard & Plé 2000 and Plé & Bayard 2001). The calculation of Eshelby's tensor for various ellipsoidal forms was programmed in SARAH. For a twinge $r_0 = 3$ (Fig. 4), we obtain:

$$S = \begin{pmatrix} 0.61 & -0.03 & 0.06 & 0 & 0 & 0 \\ -0.03 & 0.61 & 0.06 & 0 & 0 & 0 \\ 0.06 & 0.06 & 0.19 & 0 & 0 & 0 \\ 0 & 0 & 0 & 1.89 & 0 & 0 \\ 0 & 0 & 0 & 0 & 1.89 & 0 \\ 0 & 0 & 0 & 0 & 0 & 2.56 \end{pmatrix}_{\{1,2,3\}} \quad (2)$$

2.2 *Localization*

A loading in direct traction according to the direction (III) from the total reference frame is applied to the cell insulated. The strain applied to infinite is noted, ε^∞ (Fig. 4). The strains in the inclusion are given, in the global reference frame. Strains in the matrix at the inclusion-matrix interface (λ = 0) are given, in the global reference frame (Bayard & Plé 2000). Determination of the principal strains for each point M of space is done with help of the relation:

$$\det(\varepsilon - \Lambda I) = 0 \quad (3)$$

Λ is the eigenvalue of a diagonalized system. These three eigenvalues (ε_1(M), ε_2(M), ε_3(M)) are called principal strains. The associated eigenvectors are called principal direction and give information on the direction of cracking. The determination of the principal strains was carried out for various angle

values included between the direction (3) of fibres and direction (III) of loading.

The fibre concrete being a pseudo-fragile material having certain ductility, it seems preferable to approach a criterion of nucleation in strain.

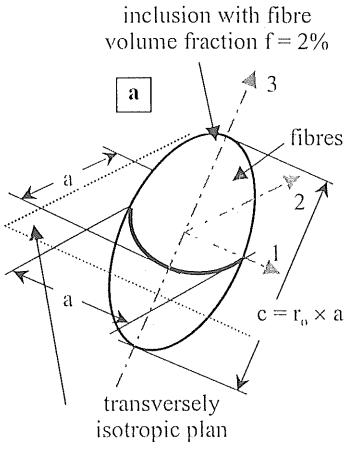

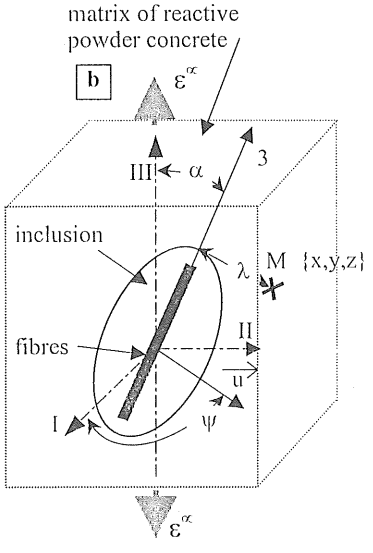

Figure 4. The inclusion model:
a) Inclusion of fibres with the symmetry axis 3 and the size of the inclusion (a × a × c) in the local reference frame (1,2,3).
b) The inclusion model : the fixed global reference frame (I,II,III) is attached to the matrix ; (1,2,3) is attached to the ellipsoidal inclusion of orientation α and ψ. The position of a point M(x,y,z) is referred by Cartesian co-ordinates (λ = 0 at inclusion-matrix interface).

We will take the criterion of Mazars in equivalent strain by:

$$\varepsilon_{eq} = \sqrt{\langle \varepsilon_1 \rangle_+^2 + \langle \varepsilon_2 \rangle_+^2 + \langle \varepsilon_3 \rangle_+^2} \qquad (4)$$

where $\langle \varepsilon_i \rangle_+$ is the deformation in extension according to direction i. We can determine, for each point M of space, the equivalent strain ε_{eq} (M). With the set of parameters { E_M = 50 GPa, ν_M = 0.18, E_f = 300 GPa, ν_f = 0.3, f = 2%, ψ = 0°, 0° < α < 90°}, the maximum tensile principal equivalent strain occurs at the inclusion-matrix interface (λ = 0).

Thus for various cases of orientation α and for a percentage out of fibres equal to 2%, we consider the distribution of the equivalent strains at interface (λ = 0). The point of nucleation, M_{crit} on the interface, checks a maximum equivalent strain (noted ε_{eq}). In this point, it is then possible to determine the principal strains, and which of maximal extension (Fig. 5). The direction of this deformation then indicates the normal to the plan of cracking to come (Fig. 6). This plane is located by angle $\theta_{fis/fib}$ between the normal to the future plan of cracking (direction of maximum extension in M_{crit}) and the direction of fibres.

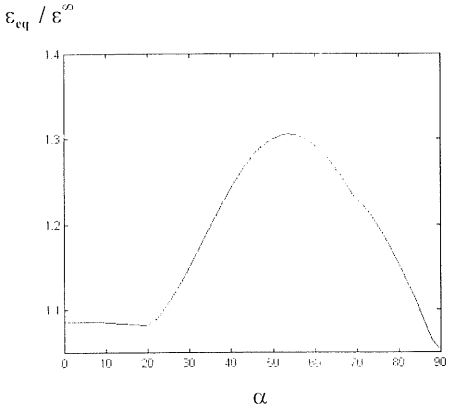

Figure 5. Maximum equivalent strain at the inclusion-matrix interface (λ = 0) for different inclinations α of the inclusion in relation ship with load direction.

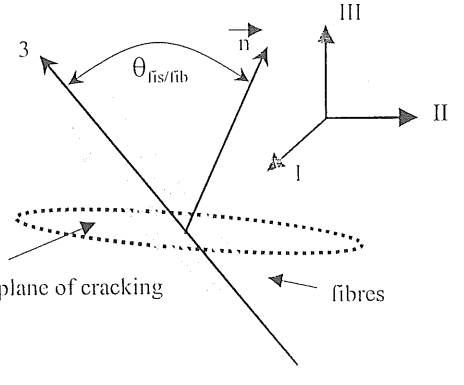

Figure 6. Crack angle $\theta_{fis/fib}$.

2.3 *Crack nucleation criterion*

A micro crack is assumed to form when the local equivalent strain (Mazars 1984) reaches the local critical equivalent strain. Restricting the analysis to cracks which form at the grain-matrix interface, the proposed criterion derives from equation (3) and (4) as:

$$\varepsilon_{eq} \geq \varepsilon_c, \forall\alpha \quad \text{with} \quad f = 2\% \tag{5}$$

We can represent the evolution of this criterion with the angle α (Fig. 7). For an inclusion of factor-form $r_0 = 3$ and with $f = 2\%$ the first crack appears when $\alpha = 54°$. In these conditions $\varepsilon_{eq}/\varepsilon_c = 0.77$, high enough to nucleate a crack if the critical equivalent strain of the matrix is equal to 1.10^{-4} (Richard & Cheyrezy 1994). This illustrates and quantifies the localisation of stresses and strains that reigns at the interface between the mass of fibres and the matrix of RPC.

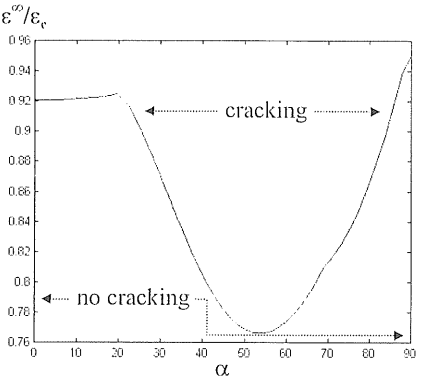

Figure 7. Crack nucleation criterion in equivalent strain.

3 DAMAGE IN THE CELL

By using the technique of the micro plans (Bazant 1984), associated with the mechanics of damage (Chaboche 1979), we can have an idea about the process of crack propagation. This type of alliance was already employed for homogenized and isotropic materials (Fichant 1996). We try here to widen the field of employment with materials with short fibres of which heterogeneity and anisotropy are taken into account. Heterogeneity is taken into account through the localization of the equivalent elastic fields, which acts on the nucleation criterion. Initial anisotropy is taken into account through transverse isotropy of inclusion of angle α. Anisotropy evolution due to induced anisotropy by cracking is translated by use of damage coupled with the micro-plans method.

To model damage of the fibre RPC, we suppose that the behaviour is mainly controlled by orientation of the reinforcement compared to the normal in the plan of cracking developed. It may be that for a given angle α, several micro-mechanisms are superimposed. Micro-mechanical description is not then easy matter to achieve. Moreover, heterogeneity related to the presence of the microscopic cracks is negligible in front of that of the fibres (Rubinstein & Xu 1990). That's why we choose to model the behaviour with phenomenological damage of manner at the scale of a cell.

3.1 *Micro plans method*

The idea consists in discretizing laws of behaviour following a certain number of plans (micro plans), defined by their normal, so to obtain for each direction of the uniaxial relations connecting the components of the strain vectors to the components of the stress vectors. This method makes it possible to take into account the triaxial behaviour of material.

This method uses a variational approximation of the stress in damaged material. To obtain the macroscopic behaviour starting from the laws of behaviour on all the micro plans, we applie a relation of the virtual type, by using a kinematic assumption (Bazant 1984), in order to guarantee the stability of the system in his lenitive behaviour. The tensor of macroscopic stresses is solution of equation of the principle of virtual work under the form:

$$\frac{4}{3}\pi\sigma\varepsilon^* = \int_{\Omega}(\sigma:\varepsilon)\,d\Omega \tag{6}$$

where Ω is the sphere of ray unit. This formulation is then supplemented by the knowledge of the laws on the micro plans connecting the normal stresses and strains as well as the tangential stress and strains. In order to simplify the problem, we will suppose for each plan, the same value binding the normal components and the tangential components. This law of specific behaviour to each plan will be related to angle which the plan considered with the direction of the fibrous reinforcement forms, $\theta_{fis/fib}$ (Fig. 6). We will consider thereafter, a relation between stress and strain calling upon a damage law of which evolution according to the imposed deformation is parameterised by angle $\theta_{fis/fib}$.

3.2 *Coupling with damage*

Contrary to the model postulating the choice of a damage tensor this formulation allows to invariability impose on the tensor of macroscopic stresses same properties of symmetry as those of the strain tensor (Fichant 1996). Instead of defining a relation between the tensors of stresses and strains, the properties are defined on each micro-plans starting from the relations between the components of σ and $\tilde{\sigma}$

(Fichant 1996). We choose to write uniaxial relations for a finished number of directions:

$$\sigma_{ij}.n_j = (1 - d(\vec{n}))\tilde{\sigma}_{ij}.n_j \quad j \in \{1,2,3\} \tag{7}$$

where $d(\vec{n})$ is a scalar variable of damage.

$$d(\vec{n}) = 1 - \exp(B_t(\varepsilon^e - \vec{n}.\varepsilon.\vec{n}) \tag{8}$$

where $B_t = B_t(\theta_{fis/fib})$ is an empirical law expressed by experimental tests.

Thus $1 - d(\vec{n})$ defines a damage surface, which makes it possible to describe anisotropy induced by cracking. This surface is approximated by an ellipsoid by defining three values of damage d_i, in three orthogonal directions. Equation (6) gives:

$$\frac{4}{3}\pi\sigma\varepsilon^* = \int_{\Omega}(1 - d(\vec{n}))\tilde{\sigma} : \varepsilon^e d\Omega \tag{9}$$

where $\tilde{\sigma}$ is the effective stress (Chaboche 1979).

It will be supposed that damage following the direction corresponding to that of fibres is minimal. On the other hand, this damage will be maximum when the fibres are placed in the plan of cracking. Indeed, when the fibres are distributed in the plan of cracking, they do not play any more the role of reinforcement and brake with respect to cracking, but worse, they constitute a defect, accelerating the damage process.

We are obliged to resort to a numerical integration process to express integrals. The convexity of potential is checked, even if the demonstration does not make object of the present article. Localization to interface inclusion evolves obviously with damage. To simplify, we supposed that the Eshelby's tensor is affected damage tensor found by the micro-plans method in the following way under the form:

$$S^{endo} = (1 - D) : S \tag{10}$$

where S^{endo} is the Eshelby's tensor of damaged cell. This tensor is equal to the initial tensor for a null damage, and the localization at the interface decreases with growing damage, with becoming equal to zero for an infinite damage ($d \rightarrow 1$).

3.3 *Results*

Orientation of cracking evolves little with damage and remains appreciably equal to that found for initial nucleation.

For an angle $\alpha = 30°$, we note an optimal couture of fibres with the weakest angle $\theta_{fis/fib}$ (Tab. 1). This is confirmed by the greatest ductility noted for the specimens thus directed.

If nucleation is one of earliest with $\alpha = 45°$, we note on the other hand that the weak angle reigning between the direction of fibres and the normal in the plan of crack $\theta_{fis/fib}$ returns damage in this case more ductile (Tab. 1). Such ductility, allows slowing down an early damage, that we could note during the tests, by a maximum effort and energy not as weak as could let it predict the criterion of nucleation.

An explanation of instability noted with $\alpha = 45°$, can come from several phenomena:

Table 1 . Crack angle evolution with α.

α	0°	30°	45°	60°	90°
$\theta_{fis/fib}$	30°	10°	23°	40°	65°

- ♦ A change of the micro-mechanisms (passage from slid-friction for weak angles to effect of belt of fibres for stronger angles),
- ♦ A possible duality of the evolutions of cracking: either cracking is born from nucleation, or cracking comes from nearby element: evolution of described by remote interaction between fibre and crack.
- ♦ The fall of the criterion of nucleation is strongest near $\alpha = 45°$ (Fig. 7), which probably goes from pair with the change of micro-mechanisms then concerned.

For an angle $\alpha = 90°$, the criterion of nucleation is strongest there with the latest cracking thus. However, absence of couture of fibres explains noted very low ductility. The behaviour is consequently fragile there as far as cracking is late (Tab. 1).

Remain that this analysis has the effect to suppose the medium damaged like infinite. Indeed, the concept of fibre to finite length intervenes in the criterion of nucleation through the method with equivalent inclusion, but does not intervene in the damage process, which touches the entire cell. This explains why orientation of cracking evolves little and does not correspond to the total profile of cracking of very whole specimens. This orientation described by the model corresponds to part of the profile of cracking. Specimen would thus have to be modeled by calling upon use of several assembled cells (Fig. 3b). This is the object of work currently in hand.

4 EXPERIMENTALE PROCEDURE

Specific specimens reinforced by oriented fibres have been tested under uniaxial tensile stress with geometry as given in Figure 8. Testing was performed in a MTS testing machine providing closed-loop servo control. A 500 kN load cell was used. The load rate was kept at 100N/s before the first crack and kept at 0.01 mm/s after. Hydraulic clamps, gripping around the ends of the specimens, were connected to the testing machine. Preliminary tests were performed on twenty samples. To obtain this samples, specific cuts were operated on a concrete

block with oriented fibres then given the orientation α equal to 0°, 30°, 45°, 60° and 90° (Fig. 8).

4.1 *Preparation of specific specimens*

The reactive powder concrete block has been prepared by BOUYGUES with a special process (Richard & Cheyrezy 1995b). A mix of reactive powder concrete with steel fibres longer than 13 mm, aggregate larger than 250 µm and a volume fraction of fibres equal to 2% were filling of the mould with compaction and through a grid to oriented fibres in the same direction (Hannant et al 1974). The concrete block has been demoulded after 48 hr given the dimensions 800 × 800 × 20 mm.

Then the samples were cut from the block using a band saw and by respecting the orientation α, then given the dimensions 700 × 50 × 20 mm (Fig. 8). Five orientations of fibres were studied (α = 0°, 30°, 45°, 60° and 90°). The uniaxial force has been measured by means of a load cell and the axial displacement has been recorded by means of LVDT extensometers placed directly on the middle part of the specimen. The load and the displacement were recorded by an automatic data acquisition system. The complete load-displacement curve is only used to determine the limit of elasticity, hardening and softening.

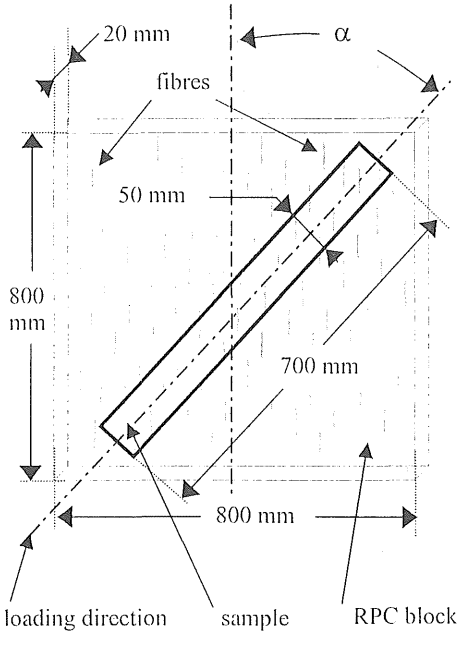

Figure 8. Reactive powder concrete block with the size of the specimen and the oriented cuts at α = 0°, 30°, 45°, 60° and 90°. Noting the loading direction in the long direction of the sample.

4.2 *Results*

The load has been applied continuously before the first crack. After, the load rate was kept at 0.01 mm/s to provide stable crack growth. After each test the orientation between the observed crack and the direction of loading was noted. A thin section of the sample, cut in a plane perpendicular to the loading direction, has been analysed (to verify the orientation of the fibres) by the help of video recording and image processing. Each images of the thin section were processed to draw automatically the contour of the fibres in the plane. The projection of the diameter of the fibres in the plane gives an ellipse, which is used to determine, with an appropriate calculation made by BOUYGUES, the orientation of fibres. Our experimental observations show the development of a pseudo-strain-hardening behaviour associated with a given orientation of fibres. When the long direction of the fibres is between $0° < \alpha < 40°$ to the direction of tension the ductile regime is always obtained (Fig. 9). When the long direction of the fibres is between $50° < \alpha < 90°$ to the tension direction, the bridging fibre action can't operate and then the material exhibits a brittle regime (Fig. 9). The transition is obtained when α is between 40° and 50°. The ul-

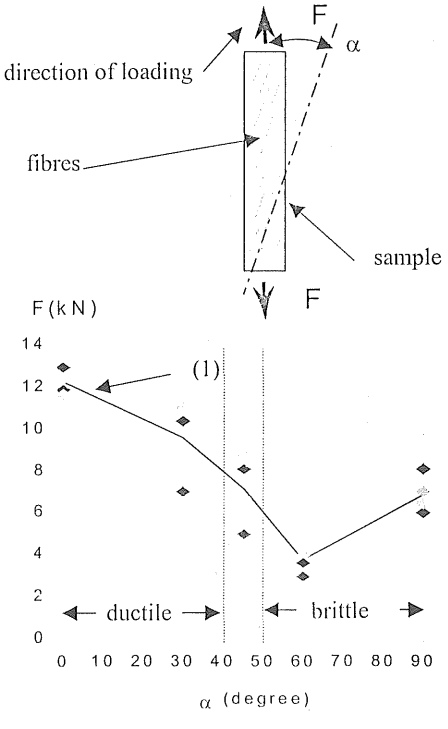

Figure 9. Experimental values of the limit of elasticity in kN in relation with the orientation of fibres. Noting the transition between the ductile and the brittle regime. The curve (1) represents the average.

timate load, in the linear part of the ascending branch of the curve (corresponding to the limit of elasticity), decreases with increasing α in the range of 0° to 60° (Fig. 9).
After this minimum value, the ultimate load increases with α (Fig. 9). In most cases, the first crack forms in the middle part of the specimen. Our observations on the orientation of the observed crack after each test show three kinds of situation. The first when the long direction of the fibres is in the loading direction (α = 0°); the observed crack is perpendicular to the tension direction but tends to propagate in the long direction of the fibres (Fig. 10). The second when α is equal to 45°; the observed crack is in the loading direction, in most cases, but tends to propagate in the long direction of the fibres (Fig. 10). And the third situation when α is equal to 90°; the observed crack is always perpendicular to the tension direction (Fig. 10).

The geometric shape of the load-displacement curve can reflect concrete toughness in some way. Our experimental value of the surface under the load-displacement curve shows a minimum average when the fibres are perpendicular to the tension direction (Fig. 11). When the orientation of the fibres is between 40° and 50°, we obtain two significant values. The first, which is the minimum value of the

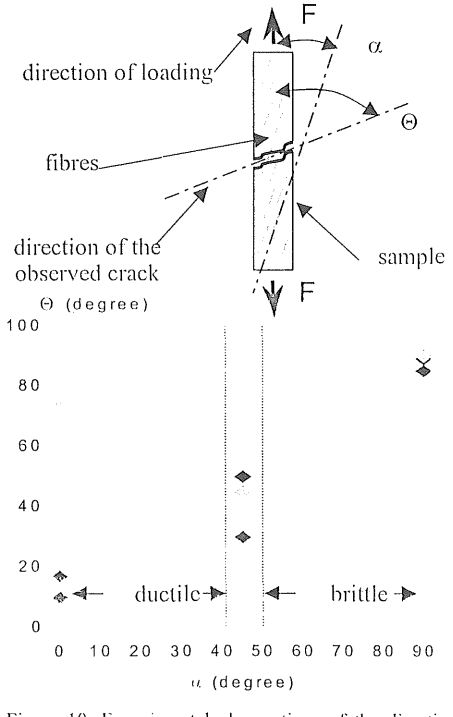

Figure 10. Experimental observations of the direction of the crack after each test in relation with the orientation of the fibres.

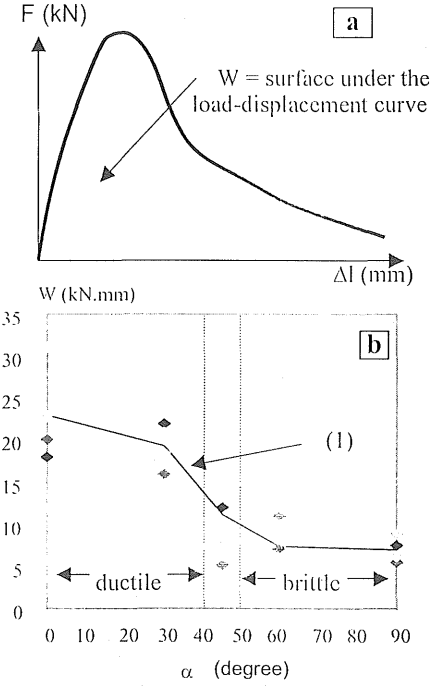

Figure 11.
a) Complete load-displacement curve.
b) Experimental values of the surface under the load-displacement curve in relation with the orientation of fibres. The curve (1) represents the average.

surface under the load-displacement curve, shows that the bridging fibre action can't operate (the crack is in the long direction of the fibres) (Fig. 11). The second value is closed to the average value obtained in the ductile regime (the bridging fibre action can operate) (Fig. 11). These observations support our theoretical analysis on the propagation of the cracks.

5 CONCLUSION

This present analysis is restricted to a linear behaviour and focuses on the formation of a crack in reactive powder concrete. A first scale modelling provides a description of the micro structural stress concentration and a model for crack initiation and crack propagation. A second scale analysis is investigated experimentally on specific samples of RPC (see above). Tensile tests in Fibre-Reinforced Concrete show the development of a pseudo-strain-hardening behaviour associated with a given orientation of fibres. With all other parameters being the same, we show experimentally that the beginning of damage process induced by anisotropy can be initiate by the first crack and control by the bridging fibre action in relation with the orientation of the fibres. These observations support our theoretical

analysis based on Eshelby's inclusion and our model of micro-plane coupled with damage theory. Our model give also some indication of the relative influence of the direction of fibres on the mechanical behaviour of RPC. Despite the restrictions that result from the preliminary nature of this small database, this shows the interest of using specific samples for fundamental studies of the processes involved in the deformation and damage of reactive powder concrete reinforced by fibres.

ACKNOWLEDGEMENT

This work is supported by the National contract Réactif/ LMT/ Bouygues/ Mécanique/ BME/ 151097. The technical help of BOUYGUES was greatly appreciated. We wish to thank Dr G. Bernier for helpful comments and discussions on the experimental procedure.

REFERENCE

Bartos, P. 1980. Analysis of pull-out tests on fibres embedded in brittle matrices. *J. Mat. Sci.* 15: 3122-3128.

Bartos, P. 1981. Review Paper : bond in fibre reinforced cements and concretes. *Int. J. Cem. Comp. & Ltwt. Concr* 3: 159-177.

Bayard, O., Plé, O. 2000. An analysis of crack nucleation in Fibre-Reinforced Concrete, in Micro Materials B. Michel T. Winkler M. Werner and H. Fecht (eds), *Simulation and Testing* 3: 718-721. Druckhaus Dresden GmbH publisher.

Bazant, Z., P. 1984. Micro plan Model for Strain-Controlled Inelastic Behaviour in C. S. Desai et al (eds), *Mechanics of engineering materials*: 45-59. John Wiley, Chichester, NY.

Bentur, A., Diamond, S. & Mindess, S. 1985. Cracking processes in steel fiber reinforced cement paste *Cem. Concr. Res.* 15: 331-342.

Bentur, A., Mindess, S. 1986. Fibre Reinforced Cementitious Composites in Applied Science. Elsevier.

Chaboche, J., L. 1979. Le concept de la contrainte effective appliqué à l'élasticité en présence d'un endommagement anisotrope, *Colloque Euromech 115*, Villars de Lans, France.

Christensen, R.M. 1979. Mechanics of composite materials in John Wiley and Sons (eds).

Cook, J. & Gordon, J. E. 1964. A mechanism for the control of crack propagation in all brittle systems in *Proc. Roy. Soc. Lond.* 282A: 508-520.

Eshelby, J.D. 1957. The determination of elastic field of an ellipsoidal inclusion and related problems in *Proc. Roy. Soc. Lond.* 241A: 376-396.

Fichant, S. 1996. Endommagement et Anisotropie induite du Béton de Structures, Thèse de doctorat de l'ENS de Cachan Paris 6.

Gray, R. J. 1984. Analysis of the effect of embedded fibre length on fibre debonding and pull-out from an elastic matrix, Part 1 : Review of theories in *J. Mat. Sci.* 19: 861-870.

Greszczuk, L. B. 1969. Theoretical studies of the mechanics of the fibre-matrix interface in composites. In Interfaces in Composites, *American Society of Testing and Materials ASTM STP* 452: 42-58. Philadelphia.

Hannant et al. 1974. Steel-fibre-reinforced mortar : a technique for producing composites with uniaxial fibre alignement *Magazine of Concrete Research* 26 (86): 47-48.

Kelly, A. & Zweben, C. 1976. Poisson contraction in aligned fibre composites showing pull-out in *J. Mat. Sci* 11: 582-587.

Majumdar. A. J. 1975. Properties of fibre reinforced composites in Fibre Reinforced Cement and Concrete A. Neville (eds), *Proc. RILEM Symp.*: 279-313. UK: The Construction Press.

Mazars, J. 1984. Application de la mécanique de l'endommagement au comportement non linéaire de la rupture du béton de structure, Thèse d'état, Univ. Paris 6.

Mura, T. 1982. Micromechanics of Defects in Solids Martinus Nijhoff (eds).

Pinchin, D. J. & Tabor, D. 1978. Interfacial contact pressure and frictional stress transfer in steel fibre cement in Proc. RILEM Conference R. N. Swamy (eds), *Testing and Test Methods of Fibre Cement Composites*: 337-344. UK: The Construction Press.

Plé, O., Bayard, O., and Alvandi, A. 2001. Preliminary study of multiscale analysis in fibre reinforced concrete in Material and Structures (refered).

Quemada, D., 1986. Rhéologie Phénoménologique des dispersions concentrées, Rheology of Heterogeneous Fluids, *Groupe Français de Rhéologie 21eme Colloque Annuel*: 1-13. Strasbourg.

Richard, P and Cheyrezy M. 1994. Reactive Powder Concrete with high ductility and 200-800 MPa compressive strength *ACI Spring Convention*. San Francisco.

Rubinstein, A., A., Xu, K. 1992. Micromechanical model of crack growth in fiber-reinforced ceramics in *J. Mech. Phys. Solids* 40 (1): 105-125.